

# Very High- $Q$ Resonant MEMS for Liquid-Phase Bio-Sensing

Hakhamanesh Mansoorzare, Sina Moradian, and Reza Abdolvand

Department of Electrical and Computer Engineering  
University of Central Florida  
Orlando, USA  
hakha@knights.ucf.edu

**Abstract**—Thin-film piezoelectric-on-silicon (TPoS) disc resonators, operating in 4-1 contour mode around 17.2 MHz, are coated with Parylene from the backside to form a biocompatible insulation layer that enables operation of the resonator in liquid media. The backsides of the resonators are chosen to be large to form a microwell that generates boundaries to the liquid assays and the diameter of such microwells is varied to allow for studying the effect of its size on the performance of the resonator under viscous damping. The results displayed very high quality factors ( $Q$ ) in water, from 315-440, that are consistently affected by the size of microwells.

**Keywords**—MEMS; disc resonator; liquid phase; biosensor;

## I. INTRODUCTION

The demand for increased accuracy and speed in drug discovery and medical diagnosis requires screening technologies with high throughput. This is particularly essential for the case of disease diagnosis where currently, complex, expensive, and bulky analyzers are employed at centralized laboratories for quantification of biomarkers of interest. Such conventional techniques despite their high accuracy, require operation by experienced technicians and often relatively long analyze time, rendering them improper for point-of-care applications [1]. In vitro assays comprising arrays of microwells and often using optical detection schemes in conjunction with labeling methods, e.g. fluorescent tagging, are increasingly employed for determining the presence and quantity of targeted cells or molecules [2]. However, the labeling process can introduce some complications such as uncertainty of results due to the invasive nature of this technique, interference in the cell binding process, and unavailability of a proper labeling agent, to name but a few. As a result, efforts have been made to develop noninvasive and label-free techniques that mostly rely on a mechanism that transforms a physical indicator associated with a targeted molecule to an electrical signal. In this regard, quartz crystal microbalances (QCM) and MEMS resonators have been widely investigated, both translating a change in their mass – due to the binding of targeted molecules – to a shift in their resonance frequency which enables a convenient readout. QCMs have shown relatively large quality factors ( $Q$ ) due to operation in shear modes, however, they suffer from miniaturization and integration issues [3]. Moreover, the large lateral dimensions of QCMs which is typically in the mm range make them improper

for detection of micron-sized targets [4]. MEMS resonators, on the other hand, are compatible with large scale integration and have very small footprints but typically suffer from substantial degradation of  $Q$  in liquid media due to energy dissipation to the liquid that either contacts the surface of resonator or fills the surrounding gaps [5, 6]. Consequently, designing a watertight resonator operating at a resonance mode with negligible out-of-plane displacement can potentially facilitate the application of MEMS resonators in bio and liquid phase sensing. Previously, we identified a resonance mode in thin-film piezoelectric-on-silicon (TPoS) disc resonators that is very immune to viscous damping [7]; the 4-1 contour mode (at 17.2 MHz) that has 8 nodes around the edge and 2 nodes along the radius. Here we have embedded such disc resonators at the bottom of waterproof microwells with different sizes that are coated with Parylene to investigate how viscous damping affects their performance as the size of the microwells is varied.

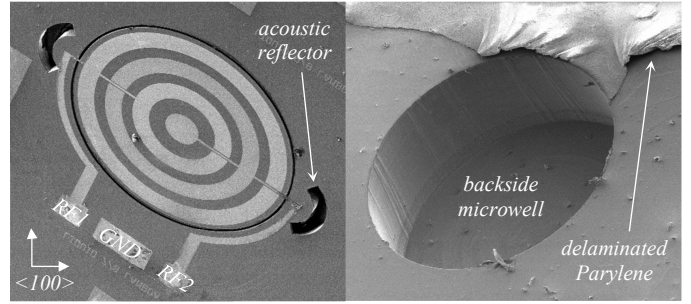


Fig. 1. Scanning electron micrograph of the topside of the disc resonator (left) and the backside of the resonator that forms the microwell for liquid insertion (right).

## II. DESIGN AND FABRICATION

TPoS disc resonators, 800  $\mu\text{m}$  in diameter, are fabricated on a Mo/Sc<sub>0.2</sub>Al<sub>0.8</sub>N/Mo/Si (0.1/1/0.1/40  $\mu\text{m}$ ) stack using an established SOI-based fabrication process flow with a minor modification prior to the final HF-release, where a thin layer of Parylene is deposited on the backside of the wafer. This way, the gaps around the released device are covered by the Parylene layer blocking the liquid from entering the gaps. The scanning electron micrograph (SEM) of the device is displayed in Fig. 1 and the fabrication process is summarized in Fig. 2. Prior to selecting this procedure, use of baked photoresist (PR) as a barrier and sacrificial layer for deposition of a planar layer of

Parylene both from the topside and backside were evaluated after the removal of the buried oxide (BOX) layer. However, due to imperfections in the PR sacrificial layer, a planar coating was not achieved and consequently, the BOX layer was chosen to be preserved before the deposition the Parylene coating. The Parylene layer is briefly exposed to oxygen plasma in order to achieve a hydrophilic surface, required for the surface wetting.

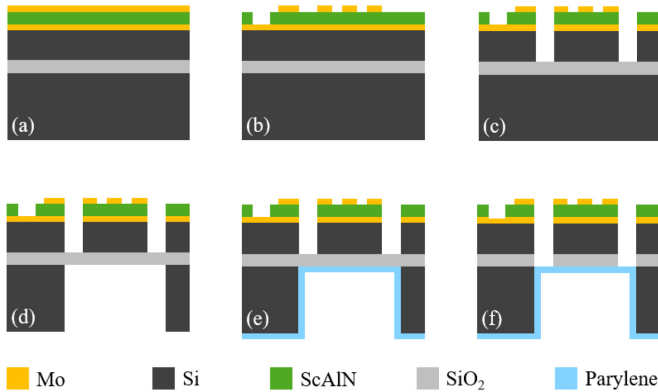


Fig. 2. Fabrication process flow showing: (a) the initial stack (b) patterning of the top electrode and contacting the bottom electrode through wet etching the piezoelectric layer (c) dry etching the device stack (d) backside DRIE to form the microwells (e) room temperature chemical vapor deposition of the Parylene coating (f) final release of the device in BOE from the topside.

The microwells for the insertion of the liquid under test are formed by the wide backside release-hole cavities and range from  $\sim 1$  mm to  $1.5$  mm in diameter with  $\sim 130$   $\mu$ m increments. The increment is chosen to be roughly 1.5 times the acoustic wavelength in water, assuming the wavelength in water is 1/5 of that in the resonator. The disc resonator is anchored to the substrate through narrow tethers directed to the [100] Si plane in order to minimize the anchor loss due to formation of displacement modal nodes (Fig. 3) that stem from the anisotropy of single crystalline Si [8]. Additionally, acoustic reflectors are etched near the tethers for further suppressing the support loss [9, 10].

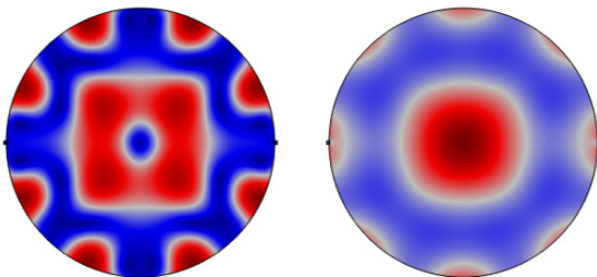


Fig. 3. Absolute displacement profile (left) and the stress profile (right) of the 4-1 contour mode obtained from COMSOL finite element analysis.

### III. MEASUREMENT RESULTS

Resonators with different microwell sizes are mounted and wire bonded on a substrate that has a hole aligned to the opening of the microwells, as depicted in Fig. 4. The substrate is flipped and the frequency response (magnitude of the transmission) of the resonators is measured using a Rohde & Schwarz ZNB 8

network analyzer at room temperature and in atmospheric pressure. Next, a syringe pump connected to a 34G syringe needle is used to fill the microwells with deionized (DI) water droplets. Surface evaporation of water from the microwells causes instability in the frequency response [11], hence, a small piece of Si is used to cover the microwells so that the vapor pressure becomes saturated quickly and a stabilized and reliable measurement be realized. The results before and after filling the microwells are summarized in Table I.

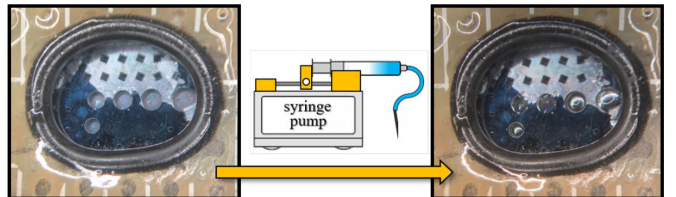


Fig. 4. Micrograph of the microwells before and after being filled with DI water.

TABLE I. INFLUENCE OF THE MICROWELL SIZE ON THE PERFORMANCE OF THE SENSOR

Diameter of microwell ( $\mu$ m)	$Q$ in air	$Q$ in water <sup>†</sup>	% decline
1460	1020	315	69
1330	915	390	57
1200	980	440	55
1070	1300	320	75

<sup>†</sup> Average once the microwells are covered and  $S_{21}$  is stabilized, repeated three times

The measurements are repeated for three times and averaged to improve the accuracy of measurements. The resonators are tested without water, with water, and finally thoroughly dried in each cycle of measurement. The measured frequency responses of the devices are plotted in Fig. 6 in the same order as shown in Table I. The highest  $Q$  that also corresponds to the least percentage degradation due to the viscous damping is observed in the device that has a microwell that is  $1200$   $\mu$ m in diameter. It has been previously demonstrated that the release area (size of the microwells in here) affects the quality factor of the resonator [12]; however, the trend of the quality factor as a function of the size of microwells is not consistent before and after insertion of water and the authors believe that such different trend could be due to the formation of damped standing waves from the body of resonator to the boundary of the microwell that enforces a fixed-free boundary condition (Fig. 5):

$$L = 0.5 \times (\text{microwell diameter} - 800) = (2n-1)\lambda/4$$

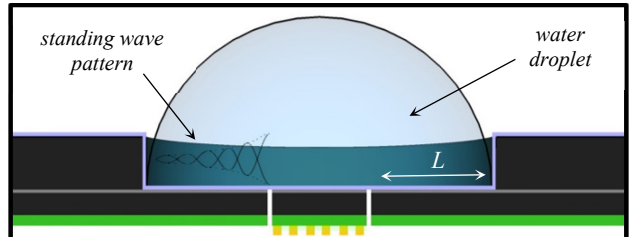


Fig. 5. Schematic of the microwell, displaying possible formation of damped standing waves in the water droplet.

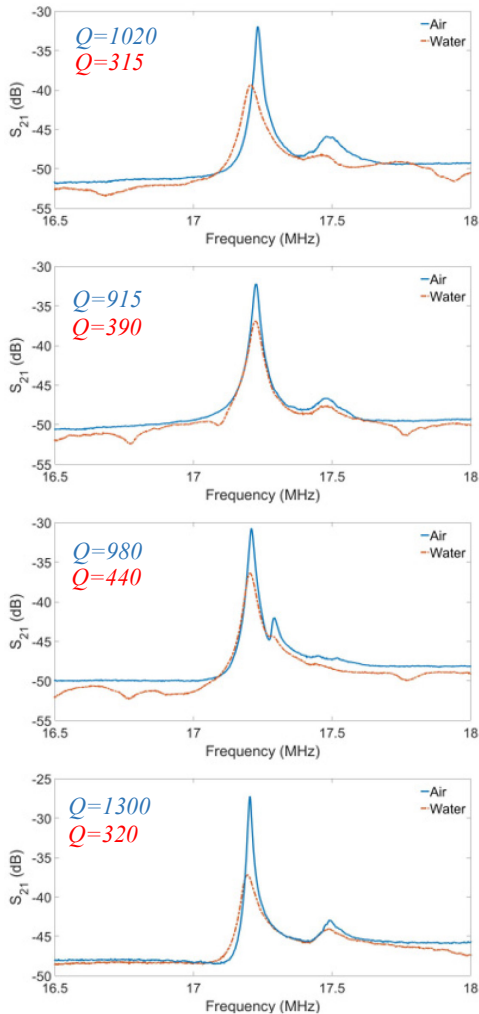


Fig. 6. Frequency response of the devices with different microwell diameters (1070  $\mu\text{m}$  - 1460  $\mu\text{m}$ ) compared in air and water.

#### IV. CONCLUSIONS

By embedding Thin-film piezoelectric-on-silicon (TPoS) disc resonators at the bottom of Parylene covered microwells that have different sizes, the effect of viscous damping on the performance of such devices were investigated. Resonators operating at 4-1 contour mode demonstrated record high quality factors (up to 440) that are directly impacted by the size of microwells. Such microwells can be used in arrays to form

microfluidic-based in vitro assays for rapid detection of targeted substances.

#### ACKNOWLEDGMENT

This work was supported by the National Science Foundation (NSF) under award 1711632.

#### REFERENCES

- [1] S. O'Sullivan, et al. "Developments in Transduction, Connectivity and AI/Machine Learning for Point-of-Care Testing." *Sensors* 19.8 (2019): 1917.
- [2] C. J. Choi, et al., "Comparison of label-free biosensing in microplate, microfluidic, and spot-based affinity capture assays." *Analytical biochemistry* 405.1 (2010): 1-10.
- [3] C. Lu, and A. W. Czanderna, eds. *Applications of piezoelectric quartz crystal microbalances*. Vol. 7. Elsevier, 2012.
- [4] W. Pang, H. Zhao, E. S. Kim, H. Zhang, H. Yu, and X. Hu. "Piezoelectric microelectromechanical resonant sensors for chemical and biological detection." *Lab on a Chip*, 12(1) (2012), 29-44.
- [5] M. Mahdavi, and S. Pourkamali. "Microresonator-on-Membrane for Real-Time Mass Sensing in Liquid Phase." *IEEE Sensors Letters* 2.3 (2018): 1-4.
- [6] A. Ali, and JE-Y. Lee. "Fully-differential Piezoelectric Button-like Mode Disk Resonator for Liquid Phase Sensing." *IEEE Transactions on Ultrasonics, Ferroelectrics, and Frequency Control* (2018).
- [7] H. Mansoorzare, S. Moradian, R. Abdolvand. "Parylene-Coated Piezoelectrically-Actuated Silicon Disc Resonators for Liquid-Phase Sensing." In *2019 Transducers & Eurosensors XXXIII: The 20th International Conference on Solid-State Sensors, Actuators and Microsystems (TRANSDUCERS & EUROSENSORS XXXIII)*. IEEE, 2019.
- [8] S. Shahraini, M. Shahmohammadi, H. Fatemi and R. Abdolvand, "Side-Supported Radial-Mode Thin-Film Piezoelectric-on-Silicon Disk Resonators," in *IEEE Transactions on Ultrasonics, Ferroelectrics, and Frequency Control*, vol. 66, no. 4, pp. 727-736, 2019.
- [9] B. P. Harrington, and R. Abdolvand. "In-plane acoustic reflectors for reducing effective anchor loss in lateral-extensional MEMS resonators." *Journal of Micromechanics and Microengineering* 21.8 (2011): 085021.
- [10] H. Mansoorzare, S. Moradian, S. Shahraini, J. Gonzales, and R. Abdolvand. "Achieving the Intrinsic Limit of Quality Factor in VHF Extensional-Mode Block Resonators." *2018 IEEE International Frequency Control Symposium (IFCS)*. IEEE, 2018.
- [11] T. Zhou, K. A. Marx, M. Warren, H. Schulze, and S. J. Brahnut. "The quartz crystal microbalance as a continuous monitoring tool for the study of endothelial cell surface attachment and growth." *Biotechnology Progress* 16.2, pp. 268-2, 2000.
- [12] B. Gibson, K. Qalandar, C. Cassella, G. Piazza, and K. L. Foster. "A study on the effects of release area on the quality factor of contour-mode resonators by laser doppler vibrometry." *IEEE Transactions on Ultrasonics, Ferroelectrics, and Frequency Control*, vol. 64, no. 5, pp. 898-904, 2017.